R-11-22

# Microbial incidence on copper and titanium embedded in compacted bentonite clay

Jörgen Persson, Sara Lydmark, Johanna Edlund
Anna Pääjärvi, Karsten Pedersen

Microbial Analytics Sweden AB

October 2011

**Svensk Kärnbränslehantering AB**
Swedish Nuclear Fuel
and Waste Management Co

Box 250, SE-101 24 Stockholm
Phone +46 8 459 84 00

ISSN 1402-3091
SKB R-11-22

# Microbial incidence on copper and titanium embedded in compacted bentonite clay

Jörgen Persson, Sara Lydmark, Johanna Edlund
Anna Pääjärvi, Karsten Pedersen

Microbial Analytics Sweden AB

October 2011

# Abstract

The incidence of bacteria on metal surfaces was examined in an experimental setting simulating conditions of the proposed Swedish concept for disposal of spent nuclear fuel. Titanium and copper rods were embedded in compacted bentonite clay saturated with groundwater collected at a depth of 450 m. Bentonite blocks were exposed to an external flux of groundwater with or without added lactate or $H_2$ for up to 203 days. Bacterial accumulation on metal rods and in the surrounding bentonite was analyzed using real-time quantitative PCR (qPCR), with genetic markers for overall bacterial presence (*16S* rDNA) as well as specific for sulfate-reducing bacteria (*apsA*). Clay species composition was analyzed by cloning and sequencing *16S* rDNA extracted from the clay. Results suggest limited bacterial accumulation on metal surfaces, amounting to a maximum of approximately $10^6$ *apsA* copies $cm^{-2}$, corresponding to a 3.7% coverage of metal surfaces. Bacterial species composition appeared to be a mix of species originating from the bentonite clay and from the added groundwater, including an apparently high proportion of sulfate-reducing bacteria. While titanium surfaces exhibited higher bacterial presence than did copper surfaces, neither the degree of bentonite compaction nor the addition of lactate or $H_2$ appeared to have any effect on the bacterial incidence on metal surfaces.

# Sammanfattning

I syfte att undersöka bakterietäckningen på metallytor under förhållanden liknande den föreslagna svenska modellen för slutförvar för använt kärnbränsle, KBS-3, analyserades mängden bakterier på koppar- och titanstavar som varit inbäddade i kompakterad, grundvattenmättad bentonit. Metallstavarna utsattes för varierande tryck- och näringsförhållanden under upp till 203 dagar innan analys av bakterieansamlingen utfördes med hjälp av kvantitativ PCR (qPCR) på såväl metallytor som på den använda bentonitleran. I syfte att uppskatta det generella bakteriebeståndet samt det specifika beståndet av sulfatreducerande bakterier användes två separata genetiska markörer, *16S* rDNA och *apsA*. Bentonitens artsammansättning analyserades vid försökets slut med hjälp av kloning och sekvensering av *16S* rDNA extraherat ur leran. Resultaten tyder på begränsad ansamling av bakterier på metallytorna, med en högsta täckning på cirka $10^6$ *apsA* kopior $cm^{-2}$, motsvarande 3.7% av metallytorna. Artsammansättningen bestod av en blandning av bakterier härstammande från bentonitleran och från det tillsatta grundvattnet, med en relativt hög andel sulfatreducerande bakterier. Titanytorna uppvisade en högre täckningsgrad än kopparytorna, medan varken bentonitens kompakteringsgrad eller tillsatser av laktat eller vätgas ($H_2$) resulterade i märkbara förändringar i bakterietäckning på metallytorna.

# Contents

# 1 Introduction

The longevity of spent nuclear fuel generated by nuclear energy production has led to the development of long-term disposal concepts designed to isolate the waste for up to the hundred thousand years required for radioactivity to decay to background levels. Currently, the favoured model involves encapsulating waste in metal canisters, which are then deposited in deep underground repositories, where they are embedded in materials such as bentonite clay, intended to function as a mechanical buffer and a barrier, limiting the inward transport of biological and chemical entities toward metal canisters and the outward movement of radionuclides from any ruptured canisters (SKB 2006).

In such disposal concepts, the integrity of the metal canister constitutes a key component of repository function, presenting the only absolute barrier to radionuclide migration (SKB 2006). The anaerobic environment of underground repositories excludes oxygenic corrosion, except in the initial phase immediately following repository closure (Kotelnikova 2002). In contrast, sulfide, a potent metal corrosive commonly found in subterranean, anaerobic environments, could significantly affect metal canister lifetime if allowed to reach canister surfaces. To properly model the extent and effect of sulfide-induced metal corrosion over the required timeframe, sulfide formation in various repository compartments as well as its transport rates toward disposal canisters must be accounted for.

Under the conditions suggested in the proposed disposal concept, sulfide will almost exclusively form through the biochemical reduction of sulfate by sulfate-reducing bacteria (SRB; Goldstein and Aizenshtat 1994). SRB have been demonstrated to be present in the proposed repository host formations (Boivin-Jahns et al. 1996, Eydal et al. 2009, Haveman and Pedersen 2002, Pedersen et al. 2008) as well as in bentonite clay (Masurat et al. 2010a, b), and several SRB species have been demonstrated to be readily adapted to proposed repository conditions (Klemps et al. 1985, Beeder et al. 1995).

Although the presence of SRB must be assumed in all repository compartments, far-field sulfide formation — occurring in the host formation, the host formation/bentonite interface, and/or in the outer parts of the bentonite buffer — is generally not considered to pose a copper corrosion threat. This is due to low sulfide concentrations found in the host formations, resulting in correspondingly slow transport of sulfide through the bentonite buffer (Eriksen and Jacobsson 1982, Pedersen 2010). In contrast, the relatively high sulfate concentrations commonly found in host formations suggests that near-field sulfide formation by SRB located in the proximal parts of the bentonite, in the bentonite/canister interface and/or at the canister surface, may present a hazard to canister integrity through sulfide-driven corrosion.

While previous studies have indicated that compaction and swelling of bentonite to the pressures used in proposed repository designs may be detrimental to bacterial survival and activity (Motamedi et al. 1996, Pedersen et al. 2000), it could be hypothesized that the bentonite/canister interface would present a more heterogenous spatial environment, allowing greater bacterial growth and nutrient fluxes than those occurring in the bulk bentonite. Moreover, canister surfaces could present an apt substratum for biofilm formation (Dogruöz et al. 2009), potentially resulting in substantial local buildup of active SRB communities.

Consequently, to properly model the potential for sulfide-induced metal canister corrosion in nuclear fuel repositories, the extent of SRB growth on metal canister surfaces must be quantified. Furthermore, such investigations must be performed under conditions simulating the proposed repository design as closely as possible.

To assess the potential for SRB growth and biofilm formation on metal canister surfaces in nuclear fuel repositories, we conducted a quantitative study under conditions very similar to those of the proposed KBS-3 underground repository design (SKB 2006). In short, titanium and copper rods were embedded in compacted bentonite, which was then saturated with groundwater sampled at a nuclear fuel repository test site located 450 m underground. Following saturation, differing nutritional scenarios were simulated by circulating groundwater with or without added lactate or $H_2$ over the bentonite for up to 203 days. At the conclusion of the experiment, the metal rod surfaces were analyzed for bacterial coating using real-time quantitative PCR (qPCR), allowing for the simultaneous determination of overall bacterial as well as specific SRB cover. This allowed analysis of the effects of metal type, swelling pressure, and

nutrient availability on bacterial growth on metal surfaces in a simulated long term disposal repository setting. Moreover, the bacterial species composition in the bentonite clay was investigated at the conclusion of the experiment. The consequences of bacterial growth dynamics for metal surfaces in the context of nutrient availability and the extensive operational period required of long term radioactive waste repositories were discussed.

# 2 Materials and methods

## 2.1 Configuration of oedometers

Stainless steel swelling pressure oedometers were used as basic experimental units, each holding six copper and six titanium rods, embedded in MX-80 bentonite (American Colloid Company, Arlington Heights, IL, USA) compacted to densities between 1,750 and 2,000 kg $m^{-3}$ in increments of 50 kg $m^{-3}$. MX-80 bentonite is a clay material exhibiting high water affinity resulting in considerable swelling upon hydration. Physical restriction of the swelling clay results in a swelling pressure reaching 5–10 MPa at 2,000 kg $m^{-3}$ packing density, with an accompanying average pore size in the nanometer range (Karnland et al. 2006). The metal rods used were 5 mm in height and 5 mm in diameter, for a total surface area of 1.18 $cm^2$. Titanium and copper rods were crafted from pure titanium or HLRW disposal canister copper, respectively. Each experimental oedometer consisted of a 20 mm high, 35 mm diameter cylindrical chamber holding the compacted bentonite blocks. Chambers were delimited at the top by a piston containing an inlet and an outlet, covered with a 40-µm-pore-size titanium filter preventing added bentonite from exiting the pressurized chamber (Pedersen 2010).

The oedometers were filled with compacted MX-80 bentonite to 75% of the cylindrical chamber height. Two holes were then drilled to allow two metal rods of either copper or titanium to be inserted on top of each other in each hole. The oedometers were then filled to 100% of the chamber height with air-dried bentonite and compacted to 1,750, 1,800, 1,850, 1,900, 1,950, or 2,000 kg $m^{-3}$. Two additional holes were then drilled through the entire depth of the bentonite, into which four copper or titanium rods were placed on top of each other.

Consequently, each oedometer contained six copper and six titanium rods; four rods of each metal were arranged in a vertical four-rod stack extending throughout the bentonite block (Figure 2-1), while the two remaining rods of each metal were arranged in a vertical two-rod stack, fully embedded in bentonite (Figure 2-1). Accordingly, two rods of each metal were completely embedded in bentonite,

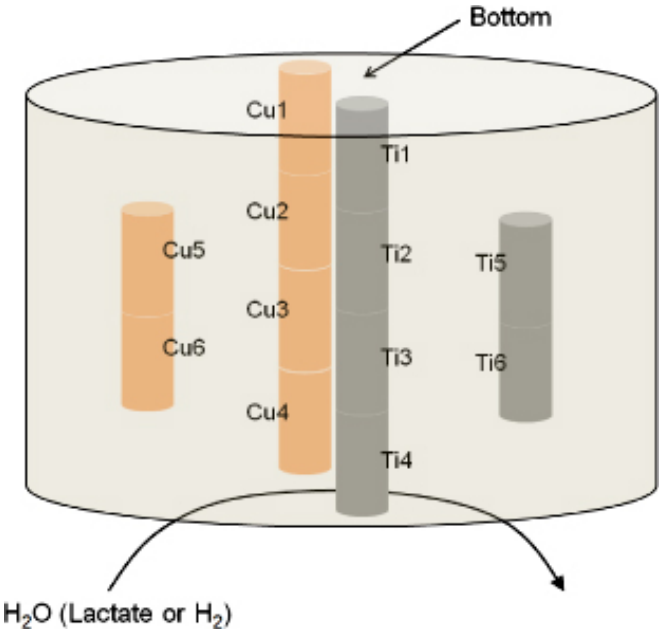


***Figure 2-1.*** *Experimental oedometer layout. Cu and Ti denote copper and titanium, respectively. Rods were stacked in four separate stacks, containing two or four rods of either copper or titanium. Stacks containing four rods were surface exposed, while the stacks containing rods 5 and 6 of each material were completely embedded in the bentonite clay. Opening the oedometers at the experiment conclusion exposed the oedometer bottom (facing upward in the image; see Figure 2-2). Water and experimental additions entered and exited oedometers at the top of the oedometer (facing downward in the image). Oedometer inner dimensions: 20×35 mm (height × diameter).*

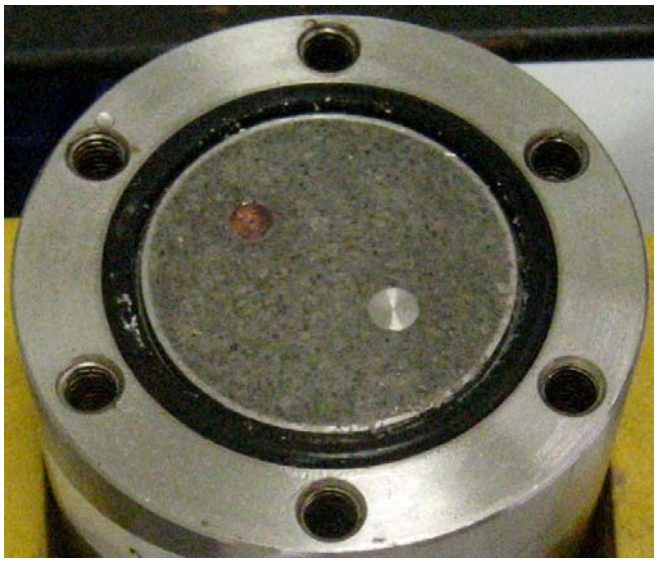

***Figure 2-2.*** *Image of oedometer immediately following opening at the conclusion of the experiment. Note the exposed metal rods (Ti1 and Cu1 in Figure 2-2). Image shows the 1,750 kg $m^{-3}$ control oedometer. Oedometer inner dimensions: 20 × 35 mm (height × diameter).*

two rods of each metal were exposed at the upper and lower faces of the compaction chambers, and the remaining two rods of each metal were stacked between surface-exposed rods, subjected to putative "piping effects" resulting from any column formed between metal rods and bentonite.

## 2.2 Experimental setup

After embedding the metal rods and compacting the bentonite, the chambers were inundated with water at 2 MPa for nine weeks. The water used for bentonite saturation and for the ensuing experimental circulations was obtained from borehole KA3510A, situated at a depth of 450 meters in the Äspö Hard Rock Laboratory in Sweden (N 57° 26.090', E 16° 39.704'). The concentrations of sulfate and sulfide in water from KA3510A have previously been determined to be 4.6 mM and 3.3 µM, respectively (Eydal et al. 2009), and the water has been found to harbor a viable SRB count of approximately $1.7 \times 10^3$ cells $mL^{-1}$ (Eydal et al. 2009).

Experimental oedometers were serially connected in three circulation systems, each holding six oedometers. Circulation in each system was maintained at approximately 20 mL $min^{-1}$ using a micropump (GAH series V21, Labinett, Göteborg, Sweden) while the flow rate was calibrated using a Promag 50 flow meter (Endress Hausser Flowtech AG, Sollentuna, Sweden); pressure data were obtained from two pressure transmitters (WIKA S-11, 40 Bar 4-20 G1/2, AB Svenska Industri Instrument, Göteborg, Sweden) fitted with digital indicators (WIKA A-A1-1 standard) installed immediately up- and downstream from each micropump (Figure 2-3).

Following water saturation of the bentonite blocks, the experimental systems were sealed and the circulation of KA3510A water at a pressure of 2 MPa over the bentonite blocks (via the oedometer inlet and outlet) commenced. Water containing no added lactate or $H_2$ was circulated through all three systems for three days, after which the systems were each dedicated to one of three experimental settings, circulating KA3510A water with no additions, or the same water containing either added lactate or added $H_2$. Additions were made using stainless steel cylinders containing hydrogen gas or a lactate solution. The cylinders were installed downstream from the oedometer series and upstream from the expansion tank (Figure 2-3) to allow for hydrogen dissolution and lactate mixing in the tank before the water reached the oedometers. The total volume of water initially circulated through the systems was 4 L for the control and hydrogen system configurations and 4.5 L for the lactate system configuration. For the lactate and $H_2$ treatments, the compounds were added to final concentrations of 14 and 10 mM, respectively. Sterilized equipment was used throughout the addition process. Following additions, circulation continued until the end of the experiment, which included intermittent sampling for circulation water analyses. The total experimental run time for the oedometers was 135–203 days (Table 2-1).

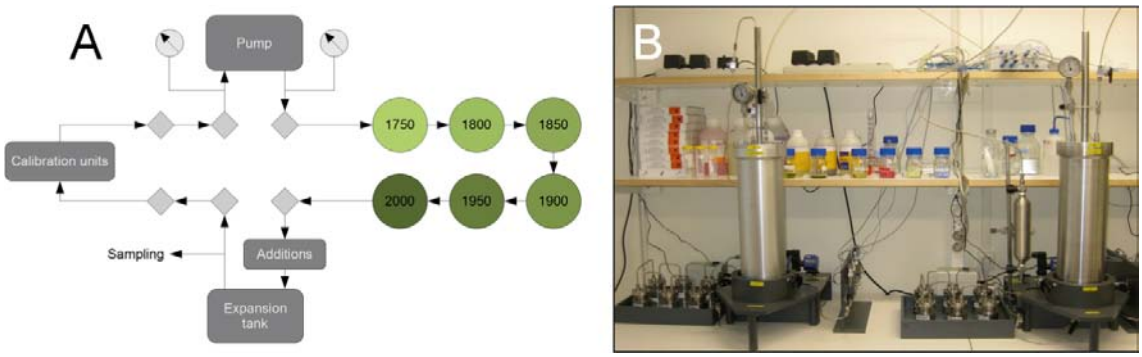


***Figure 2-3.*** *A. Schematic of the experimental system. Six oedometers were connected in series. Flow through the system was maintained by a micropump and pressure was maintained and controlled by an expansion tank and dedicated manometers. Substrates were added upstream of the expansion tank. B. Two of the systems used: control (left) and hydrogen (right).*

**Table 2-1. Oedometer sampling overview.**

| Density (kg $m^{-3}$) | Treatment | Sampling date | Experiment duration (days) |
|---|---|---|---|
| 1,750 | Lactate | 2010-01-13 | 135 |
| 1,750 | Control | 2010-01-20 | 142 |
| 1,750 | $H_2$ | 2010-01-27 | 149 |
| 1,800 | Lactate | 2010-02-03 | 156 |
| 1,800 | Control, $H_2$ | 2010-02-10 | 163 |
| 1,850 | Control, $H_2$ | 2010-02-15 | 168 |
| 1,850 | Lactate | 2010-02-22 | 175 |
| 1,900 | Control, Lactate, $H_2$ | 2010-03-08 | 189 |
| 1,950 | Control, Lactate, $H_2$ | 2010-03-15 | 196 |
| 2,000 | Control, Lactate, $H_2$ | 2010-03-22 | 203 |

## 2.3 Sampling and analysis of circulation water

Experimental circulation water was sampled for chemical, gas, and cell count analyses at 2, 4, 12, 24 and 51 days after the experimental additions. On each sampling occasion, a 150 mL sample was withdrawn from each circulation system through a valve located downstream from the expansion tank (Figure 2-2) using sterilized, anaerobic equipment. The sampled circulation water was analyzed for pH, sulfide, sulfate, acetate, lactate, $H_2$, $CO_2$, and $CH_4$ as well as for counting the total number of cells (TNC).

### 2.3.1 Water chemistry

pH was measured using a SCHOTT CG84310 pH meter equipped with a BlueLine 13 pH electrode (SI Analytics GmbH, Mainz, Germany). The electrode was calibrated according to the manufacturer's instructions. Sulfide was detected according to the $CuSO_4$ method of Widdel and Bak (1992) using a UV–visible spectrophotometer (Thermo Fisher Scientific Inc., Waltham, MA, USA). Quantification was done with reference to an external standard curve. Sulfate ($SO_4^{2-}$) concentration was determined using the SulfaVer4 method (Method #8051, HACH Lange, Sköndal, Sweden). Acetate and lactate concentrations were determined using enzymatic UV methods (Kit #10139084035 & #10148261035; R-Biopharm AG, Germany) using a Genesys 10UV spectrophotometer (Genesys, Daly City, CA, USA).

### 2.3.2 Dissolved gases

Circulation water for gas analysis was sampled into evacuated 120-mL gas flasks sealed with butyl rubber stoppers. Gas was then extracted under vacuum at room temperature and transferred to gas chromatography sample vials. $H_2$ was analyzed using a KAPPA-5/E-002 analytical gas chromatograph (AMETEK/Trace Analytical, Menlo Park, CA, USA) equipped with a 31 × 1/8-inch stainless steel molecular sieve 5A column attached to a reductive gas detector. $CO_2$ and $CH_4$ were analyzed using a Varian Star 3400CX gas chromatograph (Varian Inc., Palo Alto, CA, USA) equipped with a flame ionization detector (FID) at an oven temperature of 65°C and a detector temperature of 200°C. $CO_2$ and $CH_4$ were separated on a Porapak-Q column (2 m × 1/8 inch diameter; Sigma-Aldrich, St. Louis, MO, USA) using $N_2$ as the carrier gas, equipped with a nickel catalyst methanizer, mounted in line, to reduce $CO_2$ to $CH_4$ before detection on the FID.

### 2.3.3 Microbiology

The total number of cells (TNC) was determined using the acridine orange direct count (AODC) method as devised by Hobbie et al. (1977) and subsequently modified by Pedersen and Ekendahl (1990). Briefly described, samples were suction filtered (–20 kPa) onto 0.22-µm-pore-size Sudan black-stained polycarbonate filters, 13 mm in diameter, mounted in stainless steel analytical filter holders. The filtered cells were stained for 5–7 min with 200 µL of 10 mg $L^{-1}$ acridine orange solution, dried, and mounted between microscope slides and cover slips using fluorescence-free immersion oil. Acridine orange enters cells and associates with ribonucleic acid (RNA), in which it exhibits a maximum excitation wavelength of 460 nm, and a maximum emission wavelength of 650 nm. The number of living cells was counted under blue light (390–490 nm) and, using a band-pass filter for orange light (530 nm), in an epifluorescence microscope at 1000× magnification. At least 600 cells and 15–30 microscopic fields (1 field = 0.01 $mm^2$) were counted on each filter. Three subsamples were filtered onto three filters, which were then counted; the average of these three results was reported together with the standard deviation of the mean.

## 2.4 Sampling and analysis of bentonite and metal rods

### 2.4.1 Sampling the oedometers

To sample the metal rods and bentonite for cultivation, qPCR analysis, and cloning, each oedometer was successively disconnected from the circulation system (Figure 2-3, Table 2-1). Circulation system tubing was immediately reconnected, taking care not to allow air to enter the systems. After removal from the circulation systems, the oedometers were opened and the metal rods (Figure 2-2) were removed from the clay using sterile equipment and immediately placed in anaerobic phosphate-buffered saline (PBS) buffer. Any clay remaining on the metal rods was allowed to suspend in buffer overnight; the rods were then transferred to new PBS buffer for a final, gentle rinse before DNA extraction and analysis. Concurrently, clay samples were removed for water content analysis. Bentonite water content was determined by sampling, from each oedometer, four replicate clay samples of approximately one gram and weighing each sample before and after evaporation of water at room temperature for 48 h. The ratio of weight lost to total initial weight, expressed as a percentage, represented the clay water content. In parallel, clay was sampled for bacterial cultures and, at the centers of the three 1,850 kg $m^{-3}$ oedometers, for DNA extraction and subsequent qPCR, cloning, and sequencing.

### 2.4.2 Cultivation of sulfate-reducing bacteria

SRB cultures from bentonite clay were established by inoculating anaerobic SRB medium with a sample of clay taken near the copper or titanium rods number 5 or 6 in selected oedometers (Figure 2-1). Inoculation was performed under sterile conditions. The bentonite samples were allowed to suspend in the medium overnight at room temperature. One-mL samples of the resulting slurries were then transferred using a sulfide-flushed syringe to new anaerobic SRB medium tubes and incubated in a growth chamber according to SRB culture practices. SRB cultures exhibiting growth were extracted for DNA, from which *16S* rDNA was cloned and sequenced. The medium and procedures for SRB cultivation are described in Hallbeck and Pedersen (2008).

### 2.4.3 DNA extraction

DNA was extracted from metal rods, bentonite clay, and SRB cultures using the QIAGEN DNeasy Blood & Tissue Kit according to the manufacturer's instructions, including preparatory lysozyme treatment for Gram-positive bacteria (QIAGEN Inc., Hilden, Germany), resulting in 200-µL extracts stored at –20°C and subsequently used for qPCR and/or bacterial *16S* rDNA cloning.

### 2.4.4 Quantitative PCR determinations

To quantify bacterial cover on the metal rods, real-time quantitative PCR was performed on DNA extracted from each metal rod and from bentonite clay samples from the 1,850 kg $m^{-3}$ oedometers. Total bacterial and SRB numbers were quantified using *16S* rDNA and adenosine-5'-phosphosulfate reductase alpha subunit (*apsA*) DNA as markers, respectively. Primers used for *16S* rDNA were Q-926f and Q-1100r (Lane 1991), while *apsA* was amplified using apsAF304 and apsAR416 (Jägevall et al. 2011). For use as a quantification standard, a *Desulfovibrio aespoeensis* type 2 strain (Motamedi and Pedersen 1998) was grown and harvested in late exponential phase (Hallbeck and Pedersen 2008), its cell density being determined by a total number of cells (TNC) count. DNA extracted from this known cell density was diluted in series and subsequently used as a quantification standard in qPCR reactions. Standard dilutions used were in the range 2–5.5 × $10^5$ copies per reaction. Each qPCR reaction included a negative control with which to assess the background signal due to sample preparation as well as qPCR reactions. For *apsA* and *16S* rDNA reactions, DNA extracts from *Acetobacterium carbonolicum* (Eichler and Schink 1984) and *Methanobacterium subterraneum* (Kotelnikova et al. 1998), respectively, were used as negative controls. A negative control completely lacking DNA material was run in parallel to all samples. In all reactions, the latter control exhibited 0 copies $well^{-1}$, while the highest value recorded for DNA-containing negative controls was 13 copies $well^{-1}$.

All qPCR reactions were carried out using a Stratagene Mx3005p qPCR system (Agilent Technologies Inc., Santa Clara, CA, USA). Two and four µL of DNA extracts were used for *apsA* and *16S* rDNA reactions, respectively. All reactions contained 12.5 µL of Stratagene 2 × Brilliant II SYBR qPCR Master Mix (Cat No. 600828, Agilent Technologies Inc.). In the reactions, 0.5 µL of either *apsA* primer and 1 µL of either *16S* rDNA primer were used, for a final primer concentration of 200 nM for *apsA* primers and 400 nM for *16S* rDNA primers. In addition, 9.5 or 6.5 µL of ultrapure DNase- and RNase-free water was used for *apsA* and *16S* rDNA reactions, respectively. Total reaction volume was in all cases 25 µL. Amplification of the *16S* rRNA gene fragment was initiated by a hot start at 95°C for 10 min, followed by 45 cycles of 95°C for 30 s, 58°C for 60 s, and 72°C for 40 s. Amplification of the *apsA* gene fragment was initiated by a hot start at 95°C for 10 min, followed by 45 cycles of 95°C for 30 s, 62°C for 60 s, and 72°C for 40 s. A final melting curve analysis was carried out by continuously monitoring fluorescence between 55°C and 95°C in 0.5°C increments every 10 s. The resulting *apsA* and *16S* rDNA gene fragments were 112 and 174 base pairs in size, respectively. All qPCR reactions were run in duplicate to confirm reproducibility. In subsequent data handling, the average reported qPCR count was consistently used. All qPCR standard curves exhibited slopes between –2.9 and –3.8, intercepts between 31.4 and 36.8, and $R^2$ values >0.98. *apsA* qPCR results from the 1,750 kg $m^{-3}$ oedometer were omitted from further analyses due to the standard curve failing to adhere to quality limitations for unknown reasons.

Taking the subsampling of DNA extracts as well as the qPCR detection limit and negative control reactions into account, the qPCR quantification limit was established to be 636 copies $cm^{-2}$. In total, 122 and 169 metal rods (of a total of 216) exhibited copy counts below the quantification level of *apsA* and *16S* DNA, respectively.

qPCR quantification accuracy was assessed using parallel qPCR/TNC analyses in multiple experiments. Of the DNA extractions from metal rods harboring TNC-detectable bacterial, 58.3% produced detectable DNA, indicating a 58.3% success rate for DNA extractions. The minimum cell density detectable using qPCR was determined to be 4.0 × $10^5$ cells $cm^{-2}$, above which qPCR quantification yielded results between 1.2% and 71.5% of the cell densities recorded using TNC.

### 2.4.5 Microbial diversity in the bentonite

Microbial diversity in bentonite extracts and in cultures derived from bentonite was examined by cloning and sequencing random PCR-amplified *16S* rDNA sequences in DNA extracts. PCR reactions were performed using the broad specificity bacterial *16S* rDNA primers 27f and 1492r (Lane 1991) in 25-µL reactions. Amplifications were performed using a Bio-Rad MyCycler PCR machine and the iProof proof-reading polymerase (Bio-Rad Laboratories, Hercules, CA, USA), with an initial denaturation at 98°C for 30 s, followed by 30 cycles of denaturation at 98°C for 30 s, annealing at 60°C for 30 s, and elongation at 72°C for 40 s. The program ended with a final 5-min elongation step at 72°C. To produce 3' A-overhangs to the blunt-ended iProof polymerase products, 1 µL of Taq polymerase and additional dATP were added to the reactions, which were then incubated for an additional 30 min at 72°C.

The PCR products obtained were isolated and purified after separation on 1% agarose gels using the QIAquick Gel Extraction kit (QIAGEN Inc.) according to the manufacturer's protocol. The resulting DNA fragments were subcloned into the linearized vector pCR2.1, using the TOPO TA cloning kit (Invitrogen, San Diego, CA, USA) according to the manufacturer's protocol. The resulting plasmids were cloned into *Escherichia coli* TOP10F' cells (Invitrogen). Clones were selected for and amplified plasmids were isolated using the QIAprep Spin Miniprep kit (QIAGEN Inc.) according to the manufacturer's protocol. Inserts in isolated plasmids were sequenced by MWG Biotech (Ebersberg, Germany) using the internal *16S* rDNA primer 907r (Lane et al. 1985). The resulting sequences were aligned against known *16S* rDNA sequences in GenBank using the NCBI BLAST tool on 2010-05-06. All isolated clones exhibited a >90% similarity to database records. Isolated 16S rDNA gene sequences not exhibiting a 100% match to database records were submitted to GenBank and assigned accession numbers HQ285110 through HQ285143.

## 2.5 Data treatment

Data graphics design and statistical analyses were performed in Statistica 9.1 (Statsoft Inc., Tulsa, OK, USA). To test for statistically significant differences between groups, analysis of variance (ANOVA) followed by Tukey's Post-Hoc tests were all performed using an alpha value of 0.05. For ANOVAs regarding metal rod position effects, the data were $\log^{10}$ transformed before analysis to normalize ratios above and below 1. The qPCR quantification limit was determined to be 636 copies $cm^{-2}$. Results below this limit were considered uncertain, though they exhibited a representative distribution in the range of 0–636 copies $cm^{-2}$. Consequently, these values were included in the statistical analyses to maintain analytical power while avoiding systematic under- or overestimation of bacterial cover due to excluding values below the quantification limit or by assigning values of 0 or the lower quantification value (Helsel 1990). To confirm the ANOVA results, non-parametric statistical tests were run in parallel, using Kruskal-Wallis for comparison with the one-way ANOVA and the Friedman test to complement the two-way ANOVA. All non-parametric tests produced outcomes similar to those obtained using ANOVAs.

# 3 Results

## 3.1 Bentonite density and metal rod appearance

At the conclusion of the experiment, oedometer water content exhibited an inverse correlation with bentonite compaction (Figure 3-1), suggesting the expected proportionally decreasing pore water volume with increasing clay density. Copper rods removed from the bentonite all exhibited varying amounts of corrosion, while titanium rod surfaces appeared unaltered (Figure 3-2).

## 3.2 Circulating water

### 3.2.1 Chemistry

Circulation water composition reflected experimental treatments with respect to additions throughout the sampling period (Table 3-1). In addition, several parameters exhibited distinct changes over the analyzed time period. The pH remained stable at 6.8–7.4 throughout the experiment in the control and lactate treatments, while it increased from 7.2 to 9.0 between days 2 and 51 in the $H_2$ treatment.

While the control circulation displayed slightly decreased sulfide concentrations over time, the lactate and $H_2$ circulations exhibited marked increases from 0.07 and 0.03 µM on day 2, to 2.26 and 0.31 mM, respectively, on day 51. The sharp sulfide concentration increase in the lactate circulation was matched by a similar decrease in sulfate concentration of 1.77 mM, while the $H_2$ circulation exhibited no discernable change in sulfate concentration (Table 3-1). Parallel to the changes in sulfide concentration, the lactate circulation water displayed a marked decrease in lactate concentration from 15.8 mM on day 2 to 10.0 mM on day 51, accompanied by an increase in the concentrations of acetate and $CO_2$ from 0.1 mM and 14.0 µM to 6.4 mM and 387 µM, respectively. In contrast, the control and $H_2$ treatments exhibited slight decreases in acetate concentration over time (Table 3-1).

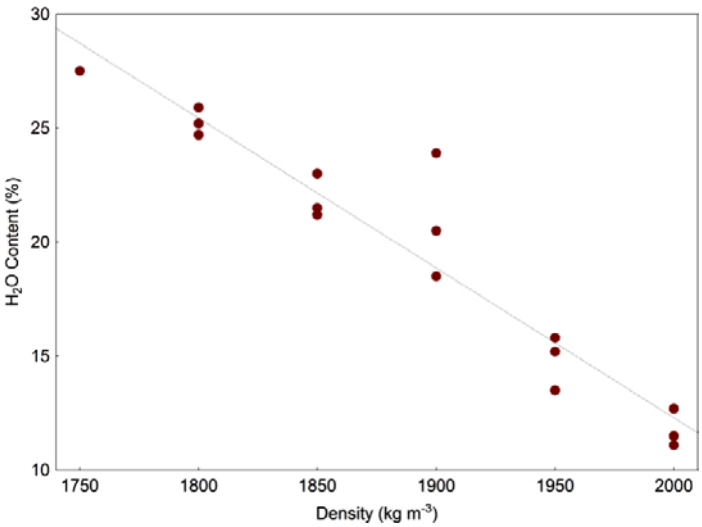


***Figure 3-1.*** *Bentonite clay water content in response to oedometer compaction. The line represents a linear regression through the sampling points ($y = 143.7–0.0657x$, $R^2 = 0.91$, $p < 0.00001$).*

**Table 3-1. Results of analyses of circulation water from the experimental systems.**

| Days after addition | Treatment | pH | Sulfide (mM) | Sulfate (mM) | Acetate (mM) | Lactate (mM) | TNC (cells $mL^{-1}$) | SD TNC (cells $mL^{-1}$) | $H_2$ (mM) | $CO_2$ (µM) | $CH_4$ (µM) |
|---|---|---|---|---|---|---|---|---|---|---|---|
| 2 | Control | 6.9 | 0.03 | 4.27 | 0.09 | 0.00 | $4.2 \times 10^4$ | $6.4 \times 10^3$ | 0 | 13 | 15.9 |
| 4 | Control | 6.8 | 0.03 | 4.17 | 0.08 | 0.00 | $6.2 \times 10^4$ | $3.3 \times 10^4$ | 0 | 12 | 15.2 |
| 12 | Control | 6.9 | 0.02 | 4.27 | 0.04 | 0.01 | $1.2 \times 10^5$ | $6.3 \times 10^4$ | 0 | 5 | 18.8 |
| 24 | Control | 7.0 | 0.01 | 5.00 | 0.05 | 0.00 | $1.1 \times 10^5$ | $9.3 \times 10^4$ | 0 | 12 | 16.9 |
| 51 | Control | 6.9 | 0.00 | 5.42 | 0.02 | 0.00 | – | – | 0 | 20 | 11.1 |
| 2 | Lactate | 7.2 | 0.07 | 3.54 | 0.13 | 15.83 | $2.5 \times 10^5$ | $1.7 \times 10^4$ | 0.1 | 14 | 24.2 |
| 4 | Lactate | 7.0 | 0.21 | 3.75 | 0.48 | 15.83 | $1.3 \times 10^6$ | $4.5 \times 10^5$ | 0 | 15 | 15.2 |
| 12 | Lactate | 6.9 | 0.91 | 3.02 | 2.54 | 12.97 | $1.1 \times 10^6$ | $4.5 \times 10^5$ | 0 | 224 | 23.9 |
| 24 | Lactate | 7.1 | 6.56 | 2.19 | 4.65 | 10.31 | $8.0 \times 10^5$ | $3.1 \times 10^5$ | 0 | 434 | 27.8 |
| 51 | Lactate | 6.9 | 2.26 | 1.77 | 6.44 | 9.96 | – | – | 0.1 | 387 | 19.0 |
| 2 | $H_2$ | 7.2 | 0.03 | 4.38 | 0.10 | 0.00 | $1.5 \times 10^4$ | $3.2 \times 10^3$ | 3.9 | 3 | 21.2 |
| 4 | $H_2$ | 7.4 | 0.04 | 4.38 | 0.10 | 0.00 | $1.2 \times 10^5$ | $3.3 \times 10^4$ | 9.1 | 3 | 20.0 |
| 12 | $H_2$ | 8.1 | 0.11 | 4.27 | 0.04 | 0.02 | $1.9 \times 10^4$ | $1.4 \times 10^4$ | >10.4 | 3 | 21.8 |
| 24 | $H_2$ | 8.4 | 0.16 | 4.79 | 0.04 | 0.00 | $3.1 \times 10^4$ | $2.0 \times 10^4$ | >10.4 | 4 | 24.6 |
| 51 | $H_2$ | 9.0 | 0.31 | 4.69 | 0.04 | 0.00 | – | – | 5.4 | 1 | 15.5 |

### 3.2.2 Gases

Hydrogen gas concentration in the $H_2$ treatment varied between 3.9 mM and >10.4 mM (the upper detection limit for $H_2$ analyses) over the 49-day sampled period. Concomitantly, $H_2$ concentration in the lactate treatment reached a maximum of 0.1 mM, while $H_2$ levels in the control experiment remained below 0.1 mM throughout the sampled period (Table 3-1). Concurrently, $CH_4$ concentrations exhibited only minor variations between treatments and sampling occasions.

### 3.2.3 Total number of cells

The TNC counts in the circulation waters indicated a significantly higher cellular density in the lactate treatment than in the control and $H_2$ treatments, throughout the sampled period from days 2 to 24 (TNC analysis failed on day 51). Thus, while the lactate treatment exhibited cell counts in the range of $2.5 \times 10^5$ to $1.3 \times 10^6$ cells $mL^{-1}$, the control and $H_2$ treatments exhibited TNC counts from $4.2 \times 10^4$ and $1.9 \times 10^4$ cells $mL^{-1}$ to $1.2 \times 10^5$ and $1.2 \times 10^5$ cells $mL^{-1}$, respectively (Table 3-1). No time-dependent trends could be detected in either treatment.

## 3.3 Metal rods and bentonite

### 3.3.1 Quantitative PCR analysis of metal rod samples

To evaluate microbial coating densities on metal rods, qPCR analyses were performed on DNA extracted from metal rod surfaces, using *apsA* DNA as a marker for SRB and bacterial *16S* rDNA as

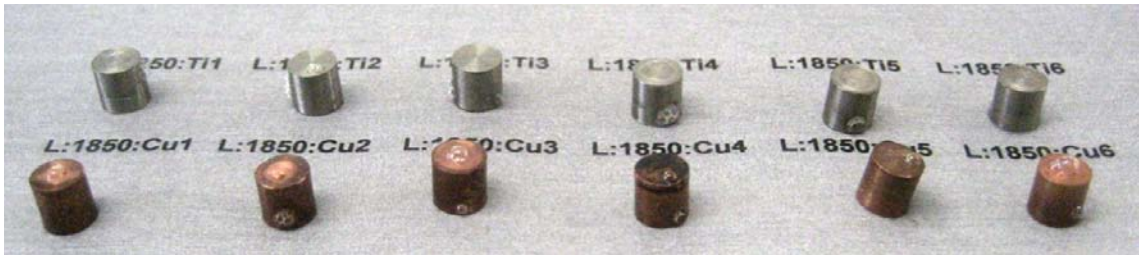


***Figure 3-2.*** *Metal rod appearance immediately after DNA extractions following removal from oedometers at the conclusion of the experiment. Image shows metal rods from the 1,850 kg $m^{-3}$ lactose treatment. Trailing numbers in the labels indicate position within oedometer (see Figure 2-2). Copper rods exhibit black discolorations.*

a marker for total bacterial presence. The highest observed *apsA* DNA copy concentrations on the surface of metal rods were $7.5 \times 10^3$ copies $cm^{-2}$ and $2.9 \times 10^3$ copies $cm^{-2}$ on titanium and copper rods, respectively, while median *apsA* DNA copy concentrations were $8.6 \times 10^2$ and $3.2 \times 10^2$ copies $cm^{-2}$ on titanium and copper rods, respectively (Table 3-2). Parallel to this, maximum *16S* DNA copy concentrations on titanium and copper rods amounted to $1.0 \times 10^4$ and $5.1 \times 10^3$ copies $cm^{-2}$, respectively. Meanwhile, median *16S* DNA copy concentrations amounted to $3.1 \times 10^2$ and $2.3 \times 10^2$ copies $cm^{-2}$ on titanium and copper surfaces, respectively (Table 3-2). DNA copy concentration exhibited relatively large variation both within and between oedometers (Figure 3-3).

When removed from the oedometers, none of the total of 216 metal rods exhibited any visually distinguishable biomass. To aid the evaluation of biomass accumulation, the maximum fraction of metal surface covered by the microbial concentration determined through qPCR analyses was calculated. Assuming a 1:1 DNA copy:cell ratio, a 1.2% qPCR quantification efficiency, a bacterial cell size of $5 \times 1 \times 1$ µm, and a single layer of bacteria on metal rod surfaces, the maximum surface coverage of bacteria on any specific metal rod would correspond to 3.7% in the present study, while median surface cover would correspond to 0.15%.

**Table 3-2. Descriptive statistics regarding DNA copy concentrations on metal rods. The unit is in all cases DNA copies $cm^{-2}$. Cu and Ti denote copper and titanium, respectively. SD and SE denote standard deviation and standard error, respectively.**

| Gene | Material | Mean | Median | SD | SE | Min | Max | n |
|---|---|---|---|---|---|---|---|---|
| apsA | Cu | 502.1 | 319.5 | 570.9 | 56.5 | 0.0 | 2,871.0 | 102 |
| | Ti | 1,015.0 | 862.0 | 1,038.5 | 102.8 | 0.0 | 7,531.0 | 108 |
| 16S | Cu | 326.7 | 234.0 | 540.9 | 52.0 | 0.0 | 5,102.0 | 108 |
| | Ti | 845.6 | 308.0 | 1,366.6 | 131.5 | 0.0 | 10,441.0 | 108 |

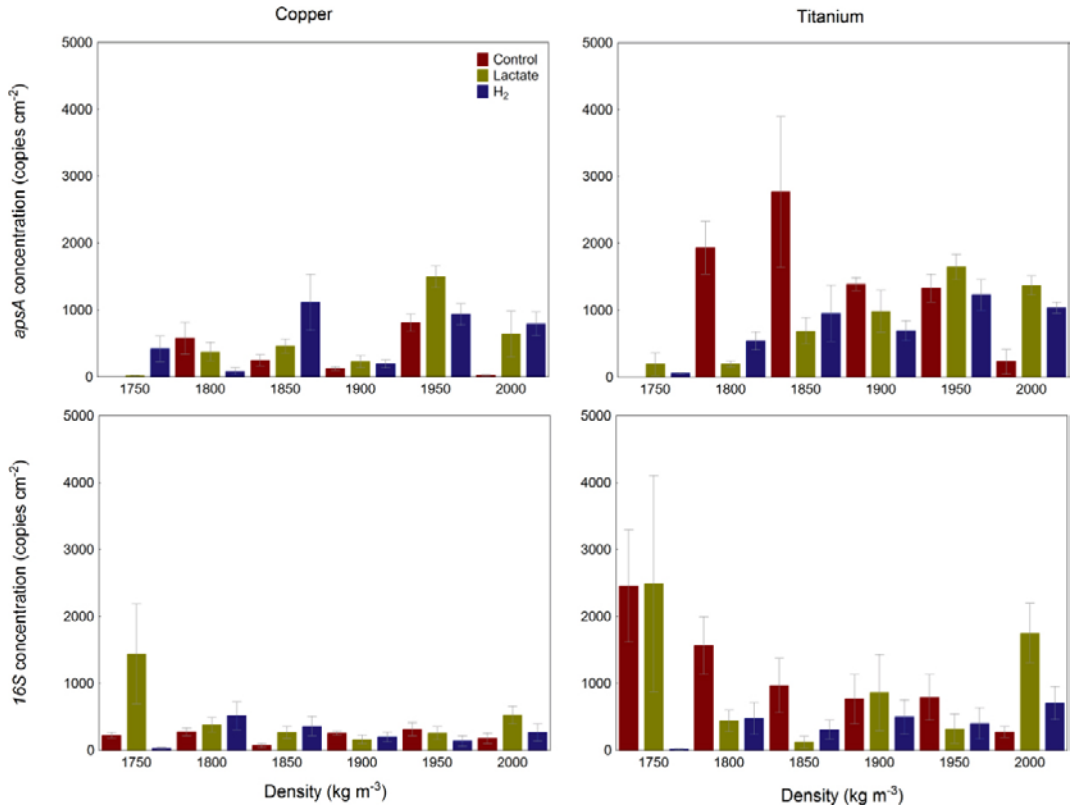


***Figure 3-3.*** *DNA copy concentrations on copper and titanium rods in various treatments. Data shown represent mean ± standard error (n = 6). Red, green, and blue bars indicate control, lactate, and $H_2$ treatments, while numbers on the horizontal axis indicate oedometer pressures.*

### 3.3.2 Quantitative PCR analysis of bentonite samples

Bentonite DNA concentrations were analyzed in three replicates using qPCR on both of the 1,850 kg $m^{-3}$ control and $H_2$ oedometers. Maximum DNA concentrations were $4.7 \times 10^3$ and $1.7 \times 10^5$ copies $g^{-1}$ clay of *apsA* and *16S* DNA, respectively, while median *apsA* and *16S* DNA copy concentrations were $6.5 \times 10^2$ and $4.1 \times 10^4$ copies $g^{-1}$ clay (Table 3-3). The specific surface area of MX-80 bentonite particles has been determined to be 31.3 $m^2$ $g^{-1}$ (Bradbury and Baeyens 2002). Consequently, the maximum copy number per $cm^2$ clay amounted to 0.02 and 0.53 copies $cm^{-2}$ for *apsA* and *16S* DNA, respectively.

### 3.3.3 Analysis of variance of qPCR data

To determine whether metal rod positioning within oedometers implies different conditions for biomass accumulation, position effects were evaluated. The positions tested for deviations were position 4, which was directly exposed water flow, and positions 2 and 3, which were subject to a putative "piping" effect due to the lack of bentonite covering rods 1–4 (Figure 2-1). Using ANOVA, these positions were tested for DNA concentration differences against rods 5 and 6, which were completely buried in bentonite. Thus, ratios between rod 4 (surface exposed) and the average of rods 5 and 6 (buried) were compared with the ratios between the average of rods 3 and 5 and the average of rods 2 and 6. Similarly, ratios between the average of rods 2 and 3 ("pipe" exposed) and the average of rods 5 and 6 (buried) were compared with the ratio of the average of rods 3 and 5 and the average of rods 2 and 6. Using this approach, no significant differences in DNA concentration were found due to positioning within oedometers (Figure 3-4), suggesting that differing exposures to circulation water did not affect the distribution of microbial biomass on metal rods.

Using one-way ANOVA, not distinguishing between oedometer densities and treatments, both *apsA* and *16S* DNA copy concentrations were demonstrated to be affected by rod material, titanium rods exhibiting significantly higher DNA concentrations than did copper rods ($p < 0.001$, $n = 102–108$). For *16S*, DNA copy concentrations amounted to 846 ± 132 and 327 ± 52 copies $cm^{-2}$ (mean ± SE) on titanium and copper rods, respectively, while for *apsA*, DNA copy concentrations were 1,015 ± $10^3$ copies $cm^{-2}$ on titanium as compared with 502 ± 57 copies $cm^{-2}$ on copper rods (mean ± SE).

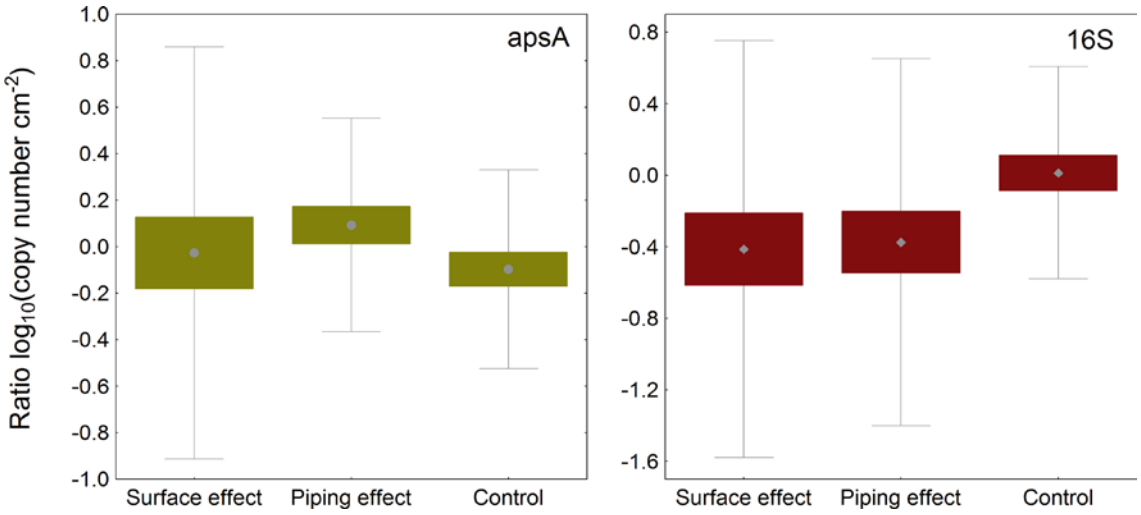


***Figure 3-4.*** *Comparison of $log_{10}$ ratios between differently positioned metal rods in oedometers. Middle points represent means, while bars represent SE and whiskers SD (n = 33–36). Higher ratios between rods 4 and the average of 5+6 or between the average of rods 2+3 and the average of 5+6 than between the average of rods 3+5 and the average of 2+6 would indicate higher DNA copy concentrations on the surface or on "pipe"-exposed rods as compared with the average oedometer DNA content.*

**Table 3-3. Descriptive statistics regarding DNA copy concentrations in bentonite clay samples from the 1,850 kg $m^{-3}$ control and $H_2$ oedometers. The unit is in all cases DNA copies $g^{-1}$ clay.**

| Marker Gene | Mean | Median | SD | SE | Min | Max | N |
|---|---|---|---|---|---|---|---|
| *apsA* | 1,139.6 | 654.4 | 1,657.9 | 676.8 | 24.6 | 4,462.5 | 6 |
| *16S* | 54,133.1 | 40,676.7 | 53,163.7 | 21,704.0 | 3,314.1 | 146,709.2 | 6 |

Two-way ANOVA was used to evaluate differences in metal rod DNA concentrations depending on experimental treatments and bentonite density. Due to the apparent difference in DNA concentrations due to rod material, titanium and copper rods were analyzed separately. While significant differences were detected between oedometers with regard to both *apsA* and *16S* copy concentrations, no discernible pattern explaining these differences could be found (Supplemental Tables A1–A4, Appendix). Thus, neither clay density nor experimental treatment (or a combination thereof) appeared to be a useful predictor of DNA copy concentration on metal rods.

### 3.3.4 Microbial diversity in the bentonite

To obtain an overview of microbial species composition in oedometers, DNA was extracted from nine microbial cultures obtained from a random series of oedometer bentonite clay samples as well as directly from the 1,850 kg $m^{-3}$ control oedometer clay. Cloning and sequencing *16S* rDNA from these samples revealed 87 clones, representing 34 apparently distinct species, several of which were detected in samples from multiple oedometers (Table 3-4). Species found include the genus *Desulfosporosinus* (obligate anaerobic, endospore-forming sulfate reducers) and *Pseudomonas stutzeri*, a denitrifying bacterium, both of which are commonly found in similar experimental systems (e.g. Chi Fru and Athar 2008). Moreover, eight distinct clones highly similar to bacteria previously found in the water used during saturation and circulation were uncovered in this study (Bacterium 060620-Aspo-KJ0052F01; Table 3-4).

**Table 3-4. 16S DNA clones detected in cultures and extractions from bentonite clay originating from 10 distinct oedometers. All detected clones exhibited more than 90% similarity to the indicated database records (accession numbers refer to database records). Accession numbers for previously undescribed clones are listed in the "Materials and Methods" section.**

| Most similar record in database | Accession # | # observations |
|---|---|---|
| *Arthrobacter globiformis* | AB098573.1 | 1 |
| *Arthrobacter oxydans* | NR_026236.1 | 3 |
| *Arthrobacter sulfonivorans* | FM955860.1 | 2 |
| Bacterium 060620-Aspo-KJ0052F01-A2-AA5 | FJ037694.1 | 4 |
| Bacterium 060620-Aspo-KJ0052F01-A6-HM13 | FJ037708.1 | 4 |
| *Clostridiaceae bacterium* | EF059534 | 1 |
| *Clostridiisalibacter paucivorans* | EF026082.1 | 3 |
| *Clostridium* sp. | AJ229251.1 | 1 |
| *Desulfosporosinus auripigmenti* | NR_025551.1 | 2 |
| *Desulfosporosinus lacus* | AJ582757.1 | 18 |
| *Desulfosporosinus* sp. | AJ582756.1 | 1 |
| *Desulfosporosinus youngii* | DQ117470.1 | 1 |
| Firmicutes bacterium | DQ833367.1 | 1 |
| *Nocardioidaceae* bacterium | AB461728.1 | 1 |
| *Paracoccus carotinifaciens* | NR_024658.1 | 1 |
| *Peptococcaceae* bacterium Y5 | AY233860.1 | 20 |
| *Pseudomonas stutzeri* | EU603456.1 | 3 |
| *Sedimentibacter hydroxybenzoicus* | NR_029146.1 | 7 |
| *Sedimentibacter* sp. | DQ168650.1 | 1 |
| *Streptomyces chungwhensis* | AY382292.2 | 2 |
| *Streptomyces monomycini* | DQ445790.1 | 1 |
| Uncultured bacterium | AB294299.1 | 2 |
| Uncultured *Sedimentibacter* sp. | EU703420.1 | 7 |
| Total | | 87 |

# 4 Discussion

The present study was undertaken to evaluate the potential for biomass accumulation on metal embedded in bentonite clay under conditions reminiscent of an underground spent nuclear fuel repository. Thus, biomass formation on titanium and copper rods was evaluated using qPCR following incubation in water-saturated bentonite clay of varying degrees of compaction and with the addition of either lactate or $H_2$ gas.

## 4.1 Activity of microorganisms in the systems

The increasing sulfide production in the circulation systems as a function of increasing reductant and carbon access strongly suggests that the experimental systems harbor active SRB. The control system circulation, containing very low concentrations of SRB-accessible electron donors, did not exhibit any noticeable SRB activity. In contrast, $H_2$- and lactate-supplemented circulations exhibited progressively increasing amounts of sulfide production over the sampled time period, the latter circulation displaying a noticeably higher activity than the former, likely reflecting the comparatively high access to carbon in the lactate circulation. Interestingly, the $H_2$ circulation exhibited a striking increase in pH over the course of sampling, indicative of $H_2$-driven sulfate reduction, a process resulting in the release of $OH^-$ (Badziong et al. 1978). Moreover, the apparent decrease in acetate concentrations in the $H_2$ circulation suggests that SRB use acetate as a carbon source for growth in this treatment.

TNC analyses of circulation water confirm the presence of bacteria in all the circulation systems (Table 3-1). Moreover, the significantly higher cell density in the lactate system as compared with the control and $H_2$ systems, together with the high sulfate-reducing activity in the lactate circulation, indicate that most bacteria in this system were SRB, for which growth was rapidly induced following lactate addition. The plateau in bacterial growth exhibited in the lactate treatment following the fourth day of sampling (despite high remaining nutrient concentrations) could indicate that groundwater-native viruses controlled bacterial growth in the circulation water (Eydal et al. 2009).

The activity of multiple SRB components suggested in the present experimental systems confirms earlier results indicating significant presence and activity of SRB from a variety of genera in MX-80 bentonite and in groundwater from the Äspö Hard Rock Laboratory test site (Chi Fru and Athar 2008, Eydal et al. 2009, Masurat et al. 2010a).

## 4.2 Numbers of microorganisms on metal rods and in bentonite

The highest DNA copy concentration detected by qPCR analyses of metal rods in the present study was 10,144 copies $cm^{-2}$ (Table 3-2). Conservatively, taking into account qPCR method variability, this constitutes 1.2% of the actual value, suggesting bacterial cell densities of $1.0 \times 10^6$ cells $cm^{-2}$. The high detected proportion of *apsA* as compared with *16S* could suggest that SRB constitute a substantial part of the biomass, although qPCR method uncertainties and varying gene copy numbers between bacterial species make such conclusions hazardous. Assuming a 1:1 ratio of DNA copies to living cells, the observed DNA copy concentrations are at the lower end of the range found in similar studies of biofilm-forming systems ($10^6$–$10^8$ cells $cm^{-2}$; Pedersen 1990, Goeres et al. 2005). The results of the present study, however, should be considered conservative (i.e. likely higher than actual) from the point of view that *apsA* and *16S* DNA are frequently present in multiple copies per cell and that DNA from dead as well as living biomass is detected using qPCR quantification.

The detected DNA copy concentrations would represent a maximum microbial surface cover on the metal rods of 3.7%, using conservative estimates of cellular size ($5 \times 1 \times 1$ µm), cellular DNA copy numbers (1 copy per cell), and cell layering (a single cell layer). Using median DNA amount as the metric, microbial metal surface cover corresponds to 0.15%. However, caution should be exercised when interpreting these results, since the relatively low success rate observed for DNA extractions

(58.3%) implies that higher cell densities may have occurred but remained undetected in the present study. A failure to retrieve DNA from metal rods would appear as a result below qPCR quantification limits, which was the observation made in 56.4% and 78.2% of the qPCR analyses for *apsA* and *16S* rDNA, respectively. In effect, results indicating copy numbers below detection levels may constitute false negatives.

The amplitude between maximum and median DNA copy numbers (by up to 34 times) illustrates the relatively high intra- and inter-oedometer variation seen in the present study (Figure 3-3). Such variation could be due to methodological variations and/or be an indication of highly spatially localized microbial distribution and growth.

Analyses of the DNA copy concentration in the bentonite clay surrounding the metal rods revealed a maximum DNA copy concentration of $1.7 \times 10^5$ copies $g^{-1}$ clay, corresponding to 0.53 copies $cm^{-2}$ clay particles, assuming an MX-80 bentonite clay-specific particle surface area of 31.3 $m^2$ $g^{-1}$ (Bradbury and Baeyens 2002). From a biological perspective, total clay particle area is less important than pore size distribution—specifically, the fraction of pores and crevices large enough to harbor microbial cells and to allow for exchange of water and nutrients with the surrounding environment. Due to uneven packing and variable particle size, clay pore size is variable (Diamond 1970, Lawrence et al. 2006) and the biologically effective specific particle area (i.e. the "inhabitable" area for microbial cells on particles) is likely much smaller than the 31.3 $m^2$ $g^{-1}$ used here. Consequently, the clay microbial concentrations determined here are likely underestimated. This is illustrated by the decreasing water content with increasing bentonite compaction, which highlights the proportionally decreasing clay pore size with increasing clay compaction (Figure 3-1).

## 4.3 Distribution of microorganisms between rods

ANOVA revealed that microbial biomass accumulation was significantly higher on titanium than on copper rods, as determined by both *apsA* and *16S* DNA copy concentrations. While this disparity could suggest that copper may negatively affect microbial growth, the observed difference may also be attributable to textural differences in metal rod surfaces or chemophysical factors affecting microbial adhesion to surfaces (Škvarla 1993), factors not controlled for in the present study.

Metal rods were positioned within oedometers to allow differential exposure of metal rods to water flowing through the oedometers following system closure (Figure 2-2). Thus, metal rod 4 and to some extent rod 1 were directly exposed to flowing water (and experimental additions), while rods 2 and 3 were interconnected to surface-exposed rods and thus putatively subject to a "piping effect". In contrast, rods 5 and 6 were completely embedded in the surrounding bentonite clay. Neither *apsA* nor *16S* DNA copy concentrations exhibited any systematic variation in response to rod position (Figure 3-4). The lack of positional effects suggests that indigenous clay microbial content and microbial dispersion by the initial water inundation (for clay saturation purposes) had significantly greater effects on microbial distribution than did water and nutrient fluxes following system closure.

The lack of changes in metal rod microbial cover in response to lactate additions stands in sharp contrast to the dramatic increase in bacterial density in the lactate treatment circulation water itself (Table 3-1, Figure 3-3). The discrepancy indicates that metal rod bacterial populations are incapable of taking advantage of the apparent nutritional advantage offered by the addition of lactate to the system. This could be due to a highly limited diffusion of specific or multiple nutrients through the bentonite toward metal rod surfaces, or to bacterial growth restricted by other physical or chemical factors, such as lack of space, low water potential, or high accumulation of growth-restricting metabolites in the bacterial near-field, induced by limited outward diffusion.

## 4.4 Diversity of microorganisms in the bentonite

The incursion of water-native microbes into the clay was apparent from the detection of eight *16S* rDNA clones identical or highly similar (Table 3-4) to bacteria specific to the water used in this study (i.e. groundwater from a borehole at a depth of 450 meters at the Äspö Hard Rock Laboratory test site, Sweden). In contrast, at least 28 of the 87 distinct clones constituted spore-forming genera

or genera previously detected in bentonite clay (Masurat 2010a), suggesting that clay-native bacteria are a substantial component of the biomass detected in this study. The overall microbial composition found in the present study was similar to that previously found in studies of the infiltration of Äspö groundwater into bentonite clay (e.g. Chi Fru and Athar 2008). Among the clones detected, several key functional groups were found, such as nitrate-reducing bacteria (*Pseudomonas stutzeri*), SRB (*Desulfosporosinus*), and obligate aerobes (*Arthrobacter*). The variety of biological niches inhabited by the detected clones suggests the potential for a variety of processes depending on the conditions to which the clay is exposed.

## 4.5 Sulfate-reducing activity in the systems

The presence of SRB has repeatedly been observed in industrial bentonite clays (e.g. Masurat et al. 2010a, b) as well as in groundwater originating at the Äspö site (Motamedi and Pedersen 1998, Hallbeck and Pedersen 2008, Eydal et al. 2009). The sulfide concentration increase in the circulation water of the lactate treatment indicate a maximum sulfide production rate under highly favourable conditions of 20.7 nmol sulfide $10^6$ cells$^{-1}$ h$^{-1}$. Applying these sulfide production rates to the cellular densities found on metal surfaces in the present study would suggest a maximum sulfide production rate of 17.5 nmol sulfide cm$^{-2}$ metal h$^{-1}$. Such production would assume that cells had unlimited access to sulfate, carbon, and electron donors (as well as other nutrients). Substrate access for bacteria embedded in bentonite will primarily be restricted by substrate transport rates through the bentonite. Accordingly, earlier studies in an experimental setup similar to the present one suggested that copper corrosion mediated by sulfide derived from sulfate reduction was dependent on substrate availability and proportional to the thickness and density of bentonite separating the copper from the sulfate source (Pedersen 2010).

Copper rods in the present study exhibited slightly corroded (blackened) surfaces upon recovery from oedometers at the conclusion of the experiment. Moreover, several oedometers revealed a distinct $H_2S$ odor when opened, in some cases accompanied by a black precipitate (indicative of FeS) in the remaining circulation water. Although these observations were not qualitatively recorded, they were indicative of ongoing sulfate reduction processes in the experimental systems.

## 4.6 Conclusions

In conclusion, the current study suggests high variation in microbial biomass accumulation on metal rods embedded in small bentonite clay volumes. Metal rod microbial cover appeared to be in the lower range of cellular densities previously detected in known biofilm-forming systems. Addition of a carbon source and electron donors to the systems appeared to have no significant effect on biomass accumulation on metal rods, while bacterial activity in the circulating water itself increased significantly with such additions. The species composition of the detected biomass appeared to be a combination of species originating from the bentonite clay and the added groundwater. Both *apsA* qPCR results and the cloning of *16S* rDNA from several sulfate-reducing genera suggest a presence of sulfate reducers on the surface of metal rods. Thus, SRB exhibit apparent viability on copper embedded in bentonite clay after compaction and water saturation. Consequently, bacterially mediated sulfate reduction could potentially occur on the surface of deposited nuclear fuel-containing copper canisters under conditions similar to those of a KBS-3 concept disposal facility.

# 5 Acknowledgements

This study was funded by the Swedish Nuclear Fuel and Waste Management Co. (SKB).

# 6 References

SKB's (Svensk Kärnbränslehantering AB) publications can be found at www.skb.se/publications.


**Badziong W, Thauer R K, Zeikus J G, 1978.** Isolation and characterization of *Desulfovibrio* growing on hydrogen plus sulphate as the sole energy source. Archives of Microbiology, 116, pp 41–49.

**Beeder J, Torsvik T, Lien T, 1995.** *Thermodesulforhabdus norvegicus* gen. nov., sp. nov., a novel thermophilic sulfate-reducing bacterium from oil field water. Archives of Microbiology, 164, pp 331–336.

**Boivin-Jahns V, Ruimy R, Bianchi A, Daumas S, Christen R, 1996.** Bacterial diversity in a deep-subsurface clay environment. Applied and Environmental Microbiology, 62, pp 3405–3412.

**Bradbury M H, Baeyens B, 2002.** Porewater chemistry in compacted re-saturated MX-80 bentonite: physico-chemical characterisation and geochemical modelling. PSI Bericht 02-10, Paul Scherrer Institute, Switzerland.

**Chi Fru E, Athar R, 2008.** In situ bacterial colonization of compacted bentonite under deep geological high-level radioactive waste repository conditions. Applied Microbiology and Biotechnology, 79, pp 499–510.

**Diamond S, 1970.** Pore size distributions in clays. Clays and Clay Minerals, 18, pp 7–23.

**Dogruöz N, Minnos B, Ilhan-Sungur E, Çotuk A, 2009.** Biofilm formation on copper and galvanized steel surfaces in a cooling-water system. IUFS Journal of Biology, 68, pp 105–111.

**Eichler B, Schink B, 1984.** Oxidation of primary aliphatic alcohols by *Acetobacterium carbinolicum* sp. nov., a homoacetogenic anaerobe. Archives of Microbiology, 140, pp 147–152.

**Eriksen T E, Jacobsson A, 1982.** Diffusion of hydrogen, hydrogen sulfide and large molecular weight anions in bentonite. SKBF/KBS TR 82-17, Svensk Kärnbränsleförsörjning AB.

**Eydal H S C, Jägevall S, Hermansson M, Pedersen K, 2009.** Bacteriophage lytic to *Desulfovibrio aespoeensis* isolated from groundwater. ISME Journal, 3, pp 1139–1147.

**Goeres D M, Loetterle L R, Hamilton M A, Murga R, Kirby D W, Donlan R M, 2005.** Statistical assessment of a laboratory method for growing biofilms. Microbiology, 151, pp 757–762.

**Goldstein T P, Aizenshtat Z, 1994.** Thermochemical sulfate reduction: a review. Journal of Thermal Analysis and Calorimetry, 42, pp 241–290.

**Hallbeck L, Pedersen K, 2008.** Characterization of microbial processes in deep aquifers of the Fennoscandian Shield. Applied Geochemistry, 23, pp 1796–1819.

**Haveman S C, Pedersen K, 2002.** Distribution of culturable microorganisms in Fennoscandian Shield groundwater. FEMS Microbiology Ecology, 39, pp 129–137.

**Helsel D R, 1990.** Less than obvious: statistical treatment of data below the detection limit. Environmental Science & Technology, 24, pp 1766–1774.

**Hobbie J E, Daley R J, Jasper S, 1977.** Use of nucleopore filters for counting bacteria by fluorescence microscopy. Applied and Environmental Microbiology, 33, pp 1225–1228.

**Jägevall S, Rabe L, Pedersen K, 2011.** Abundance and diversity of biofilms in natural and artificial aquifers of the Äspö Hard Rock Laboratory, Sweden. Microbial Ecology, 61, pp 410–422.

**Karnland O, Olsson S, Nilsson U, 2006.** Mineralogy and sealing properties of various bentonites and smectite-rich clay materials. SKB TR-06-30, Svensk Kärnbränslehantering AB.

**Klemps R, Cypionka H, Widdel F, Pfennig N, 1985.** Growth with hydrogen, and further physiological characteristics of *Desulfotomaculum* species. Archives of Microbiology, 143, pp 203–208.

**Kotelnikova S, 2002.** Microbial production and oxidation of methane in deep subsurface. Earth-Science Reviews, 58, pp 367–395.

**Kotelnikova S, Macario A J L, Pedersen K, 1998.** *Methanobacterium subterraneum* sp. nov., a new alkaliphilic, eurythermic and halotolerant methanogen isolated from deep granitic groundwater. International Journal of Systematic Bacteriology, 48, pp 357–367.

**Lane D J, 1991.** 16S/23S rDNA sequencing. In: Stackebrandt E, Goodfellow M (eds). Nucleic acid techniques in bacterial systematics. Chichester: John Wiley & Sons, pp 115–175.

**Lane D J, Pace B, Olsen G J, Stahl D A, Sogin M L, Pace N R, 1985.** Rapid determination of 16S ribosomal RNA sequences for phylogenetic analyses. Proceedings of the National Academy of Sciences of the USA, 82, pp 6955–6959.

**Lawrence G P, Payne D, Greenland D J, 2006.** Pore size distribution in critical point and freeze dried aggregates of clay subsoils. European Journal of Soil Science, 30, pp 499–516.

**Masurat P, Eriksson S, Pedersen K, 2010a.** Evidence of indigenous sulphate-reducing bacteria in commercial Wyoming bentonite MX-80. Applied Clay Science, 47, pp 51–57.

**Masurat P, Eriksson S, Pedersen K, 2010b.** Microbial sulphide production in compacted Wyoming bentonite MX-80 under *in situ* conditions relevant to a repository for high-level radioactive waste. Applied Clay Science, 47, pp 58–64.

**Motamedi M, Pedersen K, 1998.** *Desulfovibrio aespoeensis* sp. nov., a mesophilic sulfate-reducing bacterium from deep groundwater at Äspö hard rock laboratory, Sweden. International Journal of Systematic Bacteriology, 48, pp 310–315.

**Motamedi M, Karland O, Pedersen K, 1996.** Survival of sulfate reducing bacteria at different water activities in compacted bentonite. FEMS Microbiology Letters, 141, pp 83–87.

**Pedersen K, 1990.** Biofilm development on stainless steel and PVC surfaces in drinking water. Water Research, 24, pp 239–243.

**Pedersen K, 2010.** Analysis of copper corrosion in compacted bentonite clay as a function of clay density and growth conditions for sulfate-reducing bacteria. Journal of Applied Microbiology, 108, pp 1094–1104.

**Pedersen K, Ekendahl S, 1990.** Distribution and activity of bacteria in deep granitic groundwaters of southeastern Sweden. Microbial Ecology, 20, pp 37–52.

**Pedersen K, Motamedi M, Karnland O, Sandén T, 2000.** Mixing and sulphate-reducing activity of bacteria in swelling, compacted bentonite clay under high-level radioactive waste repository conditions. Journal of Applied Microbiology, 89, pp 1038–1047.

**Pedersen K, Arlinger J, Hallbeck A, Hallbeck L, Eriksson S, Johansson J, 2008.** Numbers, biomass and cultivable diversity of microbial populations relate to depth and borehole-specific conditions in groundwater from depths of 4 to 450 m in Olkiluoto, Finland. ISME Journal, 2, pp 760–775.

**SKB, 2006.** Long-term safety for KBS-3 repositories at Forsmark and Laxemar – a first evaluation. Main report of the SR-Can project. SKB TR-06-09, Svensk Kärnbränslehantering AB.

**Škvarla J, 1993.** A physico-chemical model of microbial adhesion. Journal of the Chemical Society, Faraday Transactions, 89, pp 2913–2921.

**Widdel F, Bak F, 1992.** Gram-negative mesophilic sulfate-reducing bacteria. In: Balows A, Trüper H G, Dworkin M, Harder W, Schleifer K-H (eds). The Procaryotes. New York: Springer, pp 3352–3378.

# Appendix

**Supplementary Table A-1. Matrix displaying ANOVA significance levels for differences in Ti rod *apsA* density (copy numbers $cm^{-2}$) between oedometers depending on density and experimental treatment. Numbers displayed in bold typeface denote statistically significant differences at $p < 0.05$.**

| | | 1750 | | | 1800 | | | 1850 | | | 1900 | | | 1950 | | | 2000 | | |
|---|---|---|---|---|---|---|---|---|---|---|---|---|---|---|---|---|---|---|---|
| | | Control (-) | Lactate (195.8) | $H_2$ (60.5) | Control (1933.8) | Lactate (193.5) | $H_2$ (540.0) | Control (2772.0) | Lactate (689.0) | $H_2$ (951.5) | Control (1389.5) | Lactate (983.8) | $H_2$ (694.0) | Control (1331.5) | Lactate (1651.0) | $H_2$ (1230.5) | Control (231.3) | Lactate (1368.7) | $H_2$ (1038.5) |
| **1750** | **Control (-)** | | | | | | | | | | | | | | | | | | |
| | **Lactate (195.8 )** | | | 1,0000 | 0,0501 | 1,0000 | 1,0000 | **0,0003** | 0,9998 | 0,9790 | 0,5466 | 0,9691 | 0,9998 | 0,6325 | 0,2143 | 0,7716 | 1,0000 | 0,5776 | 0,9452 |
| | **$H_2$ (60.5)** | | 1,0000 | | **0,0220** | 1,0000 | 0,9999 | **0,0002** | 0,9968 | 0,9151 | 0,3557 | 0,8898 | 0,9965 | 0,4341 | 0,1123 | 0,5818 | 1,0000 | 0,3830 | 0,8375 |
| **1800** | **Control (1933.8)** | | 0,0501 | **0,0220** | | **0,0494** | 0,2775 | 0,9476 | 0,4715 | 0,8329 | 0,9994 | 0,8658 | 0,4787 | 0,9981 | 1,0000 | 0,9895 | 0,0614 | 0,9991 | 0,9120 |
| | **Lactate (193.5)** | | 1,0000 | 1,0000 | **0,0494** | | 1,0000 | **0,0003** | 0,9998 | 0,9783 | 0,5432 | 0,9683 | 0,9998 | 0,6290 | 0,2121 | 0,7687 | 1,0000 | 0,5741 | 0,9440 |
| | **$H_2$ (540.0)** | | 1,0000 | 0,9999 | 0,2775 | 1,0000 | | **0,0019** | 1,0000 | 1,0000 | 0,9415 | 1,0000 | 1,0000 | 0,9679 | 0,6682 | 0,9913 | 1,0000 | 0,9523 | 0,9998 |
| **1850** | **Control (2772.0)** | | **0,0003** | **0,0002** | 0,9476 | **0,0003** | **0,0019** | | **0,0054** | **0,0305** | 0,2904 | **0,0372** | **0,0056** | 0,2284 | 0,6538 | 0,1436 | 0,0003 | 0,2671 | 0,0514 |
| | **Lactate (689.0)** | | 0,9998 | 0,9968 | 0,4715 | 0,9998 | 1,0000 | **0,0054** | | 1,0000 | 0,9900 | 1,0000 | 1,0000 | 0,9960 | 0,8541 | 0,9995 | 0,9999 | 0,9926 | 1,0000 |
| | **$H_2$ (951.5)** | | 0,9790 | 0,9151 | 0,8329 | 0,9783 | 1,0000 | **0,0305** | 1,0000 | | 1,0000 | 1,0000 | 1,0000 | 1,0000 | 0,9901 | 1,0000 | 0,9867 | 1,0000 | 1,0000 |
| **1900** | **Control (1389.5)** | | 0,5466 | 0,3557 | 0,9994 | 0,5432 | 0,9415 | 0,2904 | 0,9900 | 1,0000 | | 1,0000 | 0,9907 | 1,0000 | 1,0000 | 1,0000 | 0,5993 | 1,0000 | 1,0000 |
| | **Lactate (983.8)** | | 0,9691 | 0,8898 | 0,8658 | 0,9683 | 1,0000 | **0,0372** | 1,0000 | 1,0000 | 1,0000 | | 1,0000 | 1,0000 | 0,9939 | 1,0000 | 0,9798 | 1,0000 | 1,0000 |
| | **$H_2$ (694.0)** | | 0,9998 | 0,9965 | 0,4787 | 0,9998 | 1,0000 | **0,0056** | 1,0000 | 1,0000 | 0,9907 | 1,0000 | | 0,9963 | 0,8590 | 0,9995 | 0,9999 | 0,9932 | 1,0000 |
| **1950** | **Control (1331.5)** | | 0,6325 | 0,4341 | 0,9981 | 0,6290 | 0,9679 | 0,2284 | 0,9960 | 1,0000 | 1,0000 | 1,0000 | 0,9963 | | 1,0000 | 1,0000 | 0,6837 | 1,0000 | 1,0000 |
| | **Lactate (1651.0)** | | 0,2143 | 0,1123 | 1,0000 | 0,2121 | 0,6682 | 0,6538 | 0,8541 | 0,9901 | 1,0000 | 0,9939 | 0,8590 | 1,0000 | | 1,0000 | 0,2496 | 1,0000 | 0,9977 |
| | **$H_2$ (1230.5)** | | 0,7716 | 0,5818 | 0,9895 | 0,7687 | 0,9913 | 0,1436 | 0,9995 | 1,0000 | 1,0000 | 1,0000 | 0,9995 | 1,0000 | 1,0000 | | 0,8142 | 1,0000 | 1,0000 |
| **2000** | **Control (231.3)** | | 1,0000 | 1,0000 | 0,0614 | 1,0000 | 1,0000 | **0,0003** | 0,9999 | 0,9867 | 0,5993 | 0,9798 | 0,9999 | 0,6837 | 0,2496 | 0,8142 | | 0,6300 | 0,9619 |
| | **Lactate (1368.7)** | | 0,5776 | 0,3830 | 0,9991 | 0,5741 | 0,9523 | 0,2671 | 0,9926 | 1,0000 | 1,0000 | 1,0000 | 0,9932 | 1,0000 | 1,0000 | 1,0000 | 0,6300 | | 1,0000 |
| | **$H_2$ (1038.5)** | | 0,9452 | 0,8375 | 0,9120 | 0,9440 | 0,9998 | 0,0514 | 1,0000 | 1,0000 | 1,0000 | 1,0000 | 1,0000 | 1,0000 | 0,9977 | 1,0000 | 0,9619 | 1,0000 | |

**Supplementary Table A-2. Matrix displaying ANOVA significance levels for differences in Cu rod *apsA* density (copy numbers $cm^{-2}$) between oedometers depending on density and experimental treatment. Numbers displayed in bold typeface denote statistically significant differences at $p < 0.05$.**

| | | 1750 | | | 1800 | | | 1850 | | | 1900 | | | 1950 | | | 2000 | | |
|---|---|---|---|---|---|---|---|---|---|---|---|---|---|---|---|---|---|---|---|
| | | Control (-) | Lactate (16.7) | $H_2$ (418.2) | Control (577.8) | Lactate (372.8) | $H_2$ (86.3) | Control (246.2) | Lactate (457.7) | $H_2$ (1116.7) | Control (122.2) | Lactate (227.3) | $H_2$ (191.8) | Control (809.7) | Lactate (1497.3) | $H_2$ (937.5) | Control (25.2) | Lactate (641.2) | $H_2$ (791.7) |
| **1750** | **Control (-)** | | | | | | | | | | | | | | | | | | |
| | **Lactate (16.7 )** | | | 0,9722 | 0,6997 | 0,9913 | 1,0000 | 1,0000 | 0,9383 | **0,0038** | 1,0000 | 1,0000 | 1,0000 | 0,1457 | **0,0002** | 0,0375 | 1,0000 | 0,5201 | 0,1721 |
| | **$H_2$ (418.2)** | | 0,9722 | | 1,0000 | 1,0000 | 0,9959 | 1,0000 | 1,0000 | 0,3229 | 0,9989 | 1,0000 | 1,0000 | 0,9779 | **0,0050** | 0,8046 | 0,9771 | 1,0000 | 0,9859 |
| **1800** | **Control (577.8)** | | 0,6997 | 1,0000 | | 1,0000 | 0,8624 | 0,9959 | 1,0000 | 0,7580 | 0,9200 | 0,9926 | 0,9807 | 0,9999 | **0,0381** | 0,9903 | 0,7224 | 1,0000 | 1,0000 |
| | **Lactate (372.8)** | | 0,9913 | 1,0000 | 1,0000 | | 0,9993 | 1,0000 | 1,0000 | 0,2259 | 0,9999 | 1,0000 | 1,0000 | 0,9426 | **0,0027** | 0,6902 | 0,9932 | 0,9997 | 0,9596 |
| | **$H_2$ (86.3)** | | 1,0000 | 0,9959 | 0,8624 | 0,9993 | | 1,0000 | 0,9868 | **0,0097** | 1,0000 | 1,0000 | 1,0000 | 0,2671 | **0,0002** | 0,0815 | 1,0000 | 0,7167 | 0,3069 |
| **1850** | **Control (246.2)** | | 1,0000 | 1,0000 | 0,9959 | 1,0000 | 1,0000 | | 1,0000 | 0,0663 | 1,0000 | 1,0000 | 1,0000 | 0,6934 | **0,0005** | 0,3401 | 1,0000 | 0,9760 | 0,7411 |
| | **Lactate (457.7)** | | 0,9383 | 1,0000 | 1,0000 | 1,0000 | 0,9868 | 1,0000 | | 0,4232 | 0,9954 | 1,0000 | 0,9997 | 0,9922 | **0,0085** | 0,8830 | 0,9473 | 1,0000 | 0,9955 |
| | **$H_2$ (1116.7)** | | **0,0038** | 0,3229 | 0,7580 | 0,2259 | **0,0097** | 0,0663 | 0,4232 | | **0,0153** | 0,0539 | 0,0358 | 0,9983 | 0,9831 | 1,0000 | **0,0043** | 0,8905 | 0,9967 |
| **1900** | **Control (122.2)** | | 1,0000 | 0,9989 | 0,9200 | 0,9999 | 1,0000 | 1,0000 | 0,9954 | **0,0153** | | 1,0000 | 1,0000 | 0,3495 | **0,0002** | 0,1174 | 1,0000 | 0,8053 | 0,3955 |
| | **Lactate (227.3)** | | 1,0000 | 1,0000 | 0,9926 | 1,0000 | 1,0000 | 1,0000 | 1,0000 | 0,0539 | 1,0000 | | 1,0000 | 0,6411 | **0,0004** | 0,2959 | 1,0000 | 0,9636 | 0,6912 |
| | **$H_2$ (191.8)** | | 1,0000 | 1,0000 | 0,9807 | 1,0000 | 1,0000 | 1,0000 | 0,9997 | **0,0358** | 1,0000 | 1,0000 | | 0,5392 | **0,0003** | 0,2224 | 1,0000 | 0,9282 | 0,5911 |
| **1950** | **Control (809.7)** | | 0,1457 | 0,9779 | 0,9999 | 0,9426 | 0,2671 | 0,6934 | 0,9922 | 0,9983 | 0,3495 | 0,6411 | 0,5392 | | 0,3491 | 1,0000 | 0,1577 | 1,0000 | 1,0000 |
| | **Lactate (1497.3)** | | **0,0002** | 0,0050 | 0,0381 | **0,0027** | **0,0002** | **0,0005** | **0,0085** | 0,9831 | **0,0002** | **0,0004** | **0,0003** | 0,3491 | | 0,7033 | **0,0002** | **0,0773** | 0,3061 |
| | **$H_2$ (937.5)** | | **0,0375** | 0,8046 | 0,9903 | 0,6902 | 0,0815 | 0,3401 | 0,8830 | 1,0000 | 0,1174 | 0,2959 | 0,2224 | 1,0000 | 0,7033 | | **0,0414** | 0,9989 | 1,0000 |
| **2000** | **Control (25.2)** | | 1,0000 | 0,9771 | 0,7224 | 0,9932 | 1,0000 | 1,0000 | 0,9473 | **0,0043** | 1,0000 | 1,0000 | 1,0000 | 0,1577 | **0,0002** | **0,0414** | | 0,5445 | 0,1857 |
| | **Lactate (641.2)** | | 0,5201 | 1,0000 | 1,0000 | 0,9997 | 0,7167 | 0,9760 | 1,0000 | 0,8905 | 0,8053 | 0,9636 | 0,9282 | 1,0000 | 0,0773 | 0,9989 | 0,5445 | | 1,0000 |
| | **$H_2$ (791.7)** | | 0,1721 | 0,9859 | 1,0000 | 0,9596 | 0,3069 | 0,7411 | 0,9955 | 0,9967 | 0,3955 | 0,6912 | 0,5911 | 1,0000 | 0,3061 | 1,0000 | 0,1857 | 1,0000 | |

**Supplementary Table A-3. Matrix displaying ANOVA significance levels for differences in Ti rod *16S* density (copy numbers $cm^{-2}$) between oedometers depending on density and experimental treatment. Numbers displayed in bold typeface denote statistically significant differences at $p < 0.05$.**

| | | 1750 | | | 1800 | | | 1850 | | | 1900 | | | 1950 | | | 2000 | | |
|---|---|---|---|---|---|---|---|---|---|---|---|---|---|---|---|---|---|---|---|
| | | Control (2457.7) | Lactate (2492.3) | $H_2$ (20.5) | Control (1564.7) | Lactate (440.0) | $H_2$ (473.7) | Control (968.0) | Lactate (122.7) | $H_2$ (309.7) | Control (764.8) | Lactate (864.3) | $H_2$ (496.3) | Control (789.2) | Lactate (320.2) | $H_2$ (403.5) | Control (274.3) | Lactate (1752.0) | $H_2$ (707.5) |
| **1750** | **Control (2457.7)** | | 1,0000 | 0,0986 | 0,9989 | 0,3514 | 0,3811 | 0,8394 | 0,1401 | 0,2489 | 0,6650 | 0,7570 | 0,4017 | 0,6884 | 0,2564 | 0,3206 | 0,2248 | 0,9999 | 0,6086 |
| | **Lactate (2492.3)** | 1,0000 | | 0,0871 | 0,9982 | 0,3222 | 0,3507 | 0,8138 | 0,1247 | 0,2253 | 0,6313 | 0,7263 | 0,3705 | 0,6551 | 0,2323 | 0,2929 | 0,2029 | 0,9999 | 0,5741 |
| | **$H_2$ (20.5)** | 0,0986 | 0,0871 | | 0,7981 | 1,0000 | 1,0000 | 0,9977 | 1,0000 | 1,0000 | 0,9999 | 0,9994 | 1,0000 | 0,9998 | 1,0000 | 1,0000 | 1,0000 | 0,6271 | 1,0000 |
| **1800** | **Control (1564.7)** | 0,9989 | 0,9982 | 0,7981 | | 0,9847 | 0,9888 | 1,0000 | 0,8713 | 0,9571 | 0,9997 | 1,0000 | 0,9910 | 0,9998 | 0,9602 | 0,9791 | 0,9456 | 1,0000 | 0,9993 |
| | **Lactate (440.0)** | 0,3514 | 0,3222 | 1,0000 | 0,9847 | | 1,0000 | 1,0000 | 1,0000 | 1,0000 | 1,0000 | 1,0000 | 1,0000 | 1,0000 | 1,0000 | 1,0000 | 1,0000 | 0,9374 | 1,0000 |
| | **$H_2$ (473.7)** | 0,3811 | 0,3507 | 1,0000 | 0,9888 | 1,0000 | | 1,0000 | 1,0000 | 1,0000 | 1,0000 | 1,0000 | 1,0000 | 1,0000 | 1,0000 | 1,0000 | 1,0000 | 0,9497 | 1,0000 |
| **1850** | **Control (968.0)** | 0,8394 | 0,8138 | 0,9977 | 1,0000 | 1,0000 | 1,0000 | | 0,9994 | 1,0000 | 1,0000 | 1,0000 | 1,0000 | 1,0000 | 1,0000 | 1,0000 | 1,0000 | 0,9998 | 1,0000 |
| | **Lactate (122.7)** | 0,1401 | 0,1247 | 1,0000 | 0,8713 | 1,0000 | 1,0000 | 0,9994 | | 1,0000 | 1,0000 | 0,9999 | 1,0000 | 1,0000 | 1,0000 | 1,0000 | 1,0000 | 0,7249 | 1,0000 |
| | **$H_2$ (309.7)** | 0,2489 | 0,2253 | 1,0000 | 0,9571 | 1,0000 | 1,0000 | 1,0000 | 1,0000 | | 1,0000 | 1,0000 | 1,0000 | 1,0000 | 1,0000 | 1,0000 | 1,0000 | 0,8711 | 1,0000 |
| **1900** | **Control (764.8)** | 0,6650 | 0,6313 | 0,9999 | 0,9997 | 1,0000 | 1,0000 | 1,0000 | 1,0000 | 1,0000 | | 1,0000 | 1,0000 | 1,0000 | 1,0000 | 1,0000 | 1,0000 | 0,9962 | 1,0000 |
| | **Lactate (864.3)** | 0,7570 | 0,7263 | 0,9994 | 1,0000 | 1,0000 | 1,0000 | 1,0000 | 0,9999 | 1,0000 | 1,0000 | | 1,0000 | 1,0000 | 1,0000 | 1,0000 | 1,0000 | 0,9989 | 1,0000 |
| | **$H_2$ (496.3)** | 0,4017 | 0,3705 | 1,0000 | 0,9910 | 1,0000 | 1,0000 | 1,0000 | 1,0000 | 1,0000 | 1,0000 | 1,0000 | | 1,0000 | 1,0000 | 1,0000 | 1,0000 | 0,9569 | 1,0000 |
| **1950** | **Control (789.2)** | 0,6884 | 0,6551 | 0,9998 | 0,9998 | 1,0000 | 1,0000 | 1,0000 | 1,0000 | 1,0000 | 1,0000 | 1,0000 | 1,0000 | | 1,0000 | 1,0000 | 1,0000 | 0,9972 | 1,0000 |
| | **Lactate (320.2)** | 0,2564 | 0,2323 | 1,0000 | 0,9602 | 1,0000 | 1,0000 | 1,0000 | 1,0000 | 1,0000 | 1,0000 | 1,0000 | 1,0000 | 1,0000 | | 1,0000 | 1,0000 | 0,8776 | 1,0000 |
| | **$H_2$ (403.5)** | 0,3206 | 0,2929 | 1,0000 | 0,9791 | 1,0000 | 1,0000 | 1,0000 | 1,0000 | 1,0000 | 1,0000 | 1,0000 | 1,0000 | 1,0000 | 1,0000 | | 1,0000 | 0,9219 | 1,0000 |
| **2000** | **Control (274.3)** | 0,2248 | 0,2029 | 1,0000 | 0,9456 | 1,0000 | 1,0000 | 1,0000 | 1,0000 | 1,0000 | 1,0000 | 1,0000 | 1,0000 | 1,0000 | 1,0000 | 1,0000 | | 0,8478 | 1,0000 |
| | **Lactate (1752.0)** | 0,9999 | 0,9999 | 0,6271 | 1,0000 | 0,9374 | 0,9497 | 0,9998 | 0,7249 | 0,8711 | 0,9962 | 0,9989 | 0,9569 | 0,9972 | 0,8776 | 0,9219 | 0,8478 | | 0,9929 |
| | **$H_2$ (707.5)** | 0,6086 | 0,5741 | 1,0000 | 0,9993 | 1,0000 | 1,0000 | 1,0000 | 1,0000 | 1,0000 | 1,0000 | 1,0000 | 1,0000 | 1,0000 | 1,0000 | 1,0000 | 1,0000 | 0,9929 | |

**Supplementary Table A-4. Matrix displaying ANOVA significance levels for differences in Cu rod *16S* density (copy numbers $cm^{-2}$) between oedometers depending on density and experimental treatment. Numbers displayed in bold typeface denote statistically significant differences at $p < 0.05$.**

| | | 1750 | | | 1800 | | | 1850 | | | 1900 | | | 1950 | | | 2000 | | |
|---|---|---|---|---|---|---|---|---|---|---|---|---|---|---|---|---|---|---|---|
| | | Control (223.8) | Lactate (1440.7) | $H_2$ (34.7) | Control (278.0) | Lactate (381.5) | $H_2$ (516.8) | Control (72.5) | Lactate (269.3) | $H_2$ (361.3) | Control (255.7) | Lactate (160.5) | $H_2$ (200.8) | Control (314.7) | Lactate (258.2) | $H_2$ (139.7) | Control (178.2) | Lactate (525.3) | $H_2$ (268.5) |
| **1750** | **Control (-)** | | **0,0054** | 1,0000 | 1,0000 | 1,0000 | 0,9999 | 1,0000 | 1,0000 | 1,0000 | 1,0000 | 1,0000 | 1,0000 | 1,0000 | 1,0000 | 1,0000 | 1,0000 | 0,9998 | 1,0000 |
| | **Lactate (16.7 )** | **0,0054** | | **0,0006** | **0,0104** | **0,0328** | 0,1224 | **0,0009** | **0,0093** | **0,0265** | **0,0080** | **0,0025** | **0,0041** | **0,0158** | **0,0082** | **0,0019** | **0,0031** | 0,1319 | **0,0093** |
| | **$H_2$ (418.2)** | 1,0000 | **0,0006** | | 1,0000 | 0,9989 | 0,9616 | 1,0000 | 1,0000 | 0,9995 | 1,0000 | 1,0000 | 1,0000 | 0,9999 | 1,0000 | 1,0000 | 1,0000 | 0,9552 | 1,0000 |
| **1800** | **Control (577.8)** | 1,0000 | **0,0104** | 1,0000 | | 1,0000 | 1,0000 | 1,0000 | 1,0000 | 1,0000 | 1,0000 | 1,0000 | 1,0000 | 1,0000 | 1,0000 | 1,0000 | 1,0000 | 1,0000 | 1,0000 |
| | **Lactate (372.8)** | 1,0000 | **0,0328** | 0,9989 | 1,0000 | | 1,0000 | 0,9997 | 1,0000 | 1,0000 | 1,0000 | 1,0000 | 1,0000 | 1,0000 | 1,0000 | 1,0000 | 1,0000 | 1,0000 | 1,0000 |
| | **$H_2$ (86.3)** | 0,9999 | 0,1224 | 0,9616 | 1,0000 | 1,0000 | | 0,9822 | 1,0000 | 1,0000 | 1,0000 | 0,9985 | 0,9997 | 1,0000 | 1,0000 | 0,9969 | 0,9992 | 1,0000 | 1,0000 |
| **1850** | **Control (246.2)** | 1,0000 | **0,0009** | 1,0000 | 1,0000 | 0,9997 | 0,9822 | | 1,0000 | 0,9999 | 1,0000 | 1,0000 | 1,0000 | 1,0000 | 1,0000 | 1,0000 | 1,0000 | 0,9786 | 1,0000 |
| | **Lactate (457.7)** | 1,0000 | **0,0093** | 1,0000 | 1,0000 | 1,0000 | 1,0000 | 1,0000 | | 1,0000 | 1,0000 | 1,0000 | 1,0000 | 1,0000 | 1,0000 | 1,0000 | 1,0000 | 1,0000 | 1,0000 |
| | **$H_2$ (1116.7)** | 1,0000 | **0,0265** | 0,9995 | 1,0000 | 1,0000 | 1,0000 | 0,9999 | 1,0000 | | 1,0000 | 1,0000 | 1,0000 | 1,0000 | 1,0000 | 1,0000 | 1,0000 | 1,0000 | 1,0000 |
| **1900** | **Control (122.2)** | 1,0000 | **0,0080** | 1,0000 | 1,0000 | 1,0000 | 1,0000 | 1,0000 | 1,0000 | 1,0000 | | 1,0000 | 1,0000 | 1,0000 | 1,0000 | 1,0000 | 1,0000 | 1,0000 | 1,0000 |
| | **Lactate (227.3)** | 1,0000 | **0,0025** | 1,0000 | 1,0000 | 1,0000 | 0,9985 | 1,0000 | 1,0000 | 1,0000 | 1,0000 | | 1,0000 | 1,0000 | 1,0000 | 1,0000 | 1,0000 | 0,9979 | 1,0000 |
| | **$H_2$ (191.8)** | 1,0000 | **0,0041** | 1,0000 | 1,0000 | 1,0000 | 0,9997 | 1,0000 | 1,0000 | 1,0000 | 1,0000 | 1,0000 | | 1,0000 | 1,0000 | 1,0000 | 1,0000 | 0,9995 | 1,0000 |
| **1950** | **Control (809.7)** | 1,0000 | **0,0158** | 0,9999 | 1,0000 | 1,0000 | 1,0000 | 1,0000 | 1,0000 | 1,0000 | 1,0000 | 1,0000 | 1,0000 | | 1,0000 | 1,0000 | 1,0000 | 1,0000 | 1,0000 |
| | **Lactate (1497.3)** | 1,0000 | **0,0082** | 1,0000 | 1,0000 | 1,0000 | 1,0000 | 1,0000 | 1,0000 | 1,0000 | 1,0000 | 1,0000 | 1,0000 | 1,0000 | | 1,0000 | 1,0000 | 1,0000 | 1,0000 |
| | **$H_2$ (937.5)** | 1,0000 | **0,0019** | 1,0000 | 1,0000 | 1,0000 | 0,9969 | 1,0000 | 1,0000 | 1,0000 | 1,0000 | 1,0000 | 1,0000 | 1,0000 | 1,0000 | | 1,0000 | 0,9960 | 1,0000 |
| **2000** | **Control (25.2)** | 1,0000 | **0,0031** | 1,0000 | 1,0000 | 1,0000 | 0,9992 | 1,0000 | 1,0000 | 1,0000 | 1,0000 | 1,0000 | 1,0000 | 1,0000 | 1,0000 | 1,0000 | | 0,9989 | 1,0000 |
| | **Lactate (641.2)** | 0,9998 | 0,1319 | 0,9552 | 1,0000 | 1,0000 | 1,0000 | 0,9786 | 1,0000 | 1,0000 | 1,0000 | 0,9979 | 0,9995 | 1,0000 | 1,0000 | 0,9960 | 0,9989 | | 1,0000 |
| | **$H_2$ (791.7)** | 1,0000 | **0,0093** | 1,0000 | 1,0000 | 1,0000 | 1,0000 | 1,0000 | 1,0000 | 1,0000 | 1,0000 | 1,0000 | 1,0000 | 1,0000 | 1,0000 | 1,0000 | 1,0000 | 1,0000 | |